Hindawi
Geofluids
Volume 2022, Article ID 5295172, 10 pages
https://doi.org/10.1155/2022/5295172

Research Article

Coupling Analysis of Water Injection Softening-Precursor Information Prediction of Coal-Rock Mass Based on Energy Conduction

Haidong Xu[1] **Xingping Lai**[1,2] **Jiantao Cao,**[1] **Huicong Xu**[1,2] **and Shuai Zhang**[1,2]

[1]*School of Energy Resources, Xi'an University of Science and Technology, Xi'an 710054, China*
[2]*State Key Laboratory of Coal Green and Safety Development in West China, Xi'an 710054, China*

Correspondence should be addressed to Haidong Xu; 20103077005@stu.xust.edu.cn and Huicong Xu; xhcxust@163.com

Received 12 January 2022; Revised 13 March 2022; Accepted 21 April 2022; Published 21 June 2022

Academic Editor: Mingdong Wei

To further refine the rationality of pressure relief measures, the pressure relief measures are transformed from engineering scale to laboratory scale. In this paper, the static load is applied by uniaxial compression, and the difference in the energy evolution process of loaded coal samples is compared using pressure relief at an indoor scale. The test results show that the pressure relief state of water injection can meet the conditions well and reduce the impact tendency of the whole coal samples. In addition, try to analyze the reasons why it is difficult to accurately predict the formation of rockburst in coal roadway by analytical means. Due to the special structure of coal, it can be found that both natural and saturated conditions can meet the conditions in the state of water injection and pressure relief, while in the dry state, the conditions cannot be met; that is, the precursor signals of disaster cannot be accurately picked up, and finally, the failure of coal samples cannot be accurately predicted. However, on the laboratory scale, the natural coal samples are in the state of adsorption in the air after sampling, and the coal bodies near the deep underground working face tend to have low water content due to the development of pores and fissures and the influence of self-weight of mining disturbance. The research in this paper provides theoretical support for the subsequent determination of pressure relief parameters, and the related research conclusions are of great significance.

1. Introduction

According to the authority forecast, in the future, for quite a period, coal resources in China's energy consumption structure still occupy an extremely important position [1]. With the deep mining of coal resources in China, frequent dynamic disasters seriously restrict the safe mining and stable supply of coal [2–3], of which rock bursts are the most prominent [4–5]. Scholars at home and abroad have carried out extensive research to solve this worldwide problem, mainly focusing on the following three aspects [6–9]: firstly, while improving the current mechanism of rockburst, new theories are still deeply excavated to attempt to reliably describe the formation mechanism of rockburst and to inversion the whole process characteristics of rockburst gestating. Secondly, taking into account the formation of rockburst and high-stress concentration has an inevitable connection, by studying the stability of surrounding rock under various pressure relief measures and through a variety of commonly used monitoring equipment to evaluate a variety of pressure relief measures. Thirdly, the failure of coal-rock samples is a highly nonlinear process, and a single evaluation index is often unable to effectively invert the whole failure process. It is bound to require methods such as big data, cloud mining, and artificial intelligence. At the same time, the reliable pregnant disaster signals that identify the damage precursors are mainly concentrated in the collection of multiple physical quantities, which provides the basis for further study of pregnant disaster signals. The application of mature theory to the actual underground engineering scale also provides strong evidence for on-site disaster prevention and prediction. However, a rock burst involves many factors and its mechanism is complex. [10–11]. It brings unprecedented challenges to deep mineral resource mining and underground engineering maintenance, which needs further research.

The essence of rockburst is the differential distribution of energy caused by mining disturbance and the inevitable result of the dynamic adjustment in the process of quantitative change [12–13]. The existing energy priming theory shows [14–17] that the formation of rockburst is often highly correlated with the dynamic-static combination. Combined with the actual working conditions, it can be divided into static load-oriented and dynamic load-oriented. The energy start-up type of rockburst dominated by the static load is as follows: the stress of coal near the working face is highly concentrated and reaches the critical stable value. At this time, a slight disturbance can induce a rockburst. The energy start-up type of rockburst dominated by the dynamic load is shown as follows: the coal near the working face is in the normal ground stress support area. At this time, a large dynamic load is needed, which often corresponds to the fracture of the hard roof. According to the above two types of rockburst energy start-up, targeted rockburst prevention measures are proposed, which effectively guide the pressure relief measures in the project.

Considering that all the occurrence conditions of rock burst have the participation of static load, to clarify the determinants of static load, firstly, this paper applies the static load through uniaxial compression and reveals the difference in the energy evolution process of coal samples under different water injection softening and pressure relief conditions and tries to analyze the reason that it is difficult to predict the rockburst of coal roadway under the analysis method. It provides a basis for the subsequent reasonable setting of pressure relief measures and the ultimate prevention of rock bursts.

2. Experimental Scheme

The existing theoretical and practical studies have proved that water injection, blasting, and large-diameter pressure relief can effectively release the stress concentration of surrounding rock and further transfer it to the deep [18–21]. The above different measures have been optimized in the continuous practice process, and certain theoretical results have been achieved. Now, China has formed more systematic rockburst prevention measures; the prevention of rockburst has played a vital role. However, many analysis methods lack a strong theoretical basis, and coal mines often rely more on experience to determine specific implementation parameters in the process of field practice [22–25].

2.1. Description and Preparation of Coal Samples. The sampling sites of coal samples used in this experiment were all from Maiduoshan Coal Mine. According to the ISRM test standard, we processed $50\,\mathrm{mm} \times 50\,\mathrm{mm} \times 50\,\mathrm{mm}$ square coal samples. The surface of the coal sample is smooth without obvious cracks, and the cut coal sample is polished with fine sandpaper to ensure that both ends are parallel.

2.1.1. Water Injection Pressure Relief (Different Moisture Contents). To simulate the actual working conditions of water injection pressure relief, coal samples with different water contents were artificially set in the laboratory by changing the immersion time. According to different soaking times, coal samples in the dry state, natural state, and saturated state were prepared. The sample number and different water content states are shown in Table 1.

2.2. Experimental Equipment and Methods. This experiment selects an RMT-150B rock mechanics experiment machine to provide static load. The axial strain is measured by connecting the strain gauge to the DH3823 distributed signal test and analysis system. To invert the whole failure process of the loaded coal sample, the acoustic emission instrument was also used in this experiment to collect the acoustic emission signals of the whole loading process of the coal sample in real time. For the convenience of analysis, all devices in this experiment need to ensure time synchronization. To ensure that the rock sample was suddenly broken, the rock sample was stably loaded by controlling the stress in this experiment, and the loading rate was constant at 0.2 kN/s.

The testing machine is mainly composed of four parts: host, hydraulic source, DTC controller, computer data processing system, etc. The testing machine adopts an electro-hydraulic servo control system, and the driving program is a motor-hydraulic pump-servo valve-main cylinder piston-polished rod/test bench/compression fixture. The testing machine can test the basic parameters of rock mechanics such as compression, splitting, shearing, and bending (three-point bending) of rocks, coal, and concrete. The corresponding curves of stress, displacement, deformation, and time can be recorded in real time.

3. Mechanical Properties of Bearing Coal Sample Underwater Injection Softening

3.1. Mechanical Parameters of Coal Samples with Different Water Injection Softening States. In this experiment, uniaxial compression tests were conducted on coal samples under different water injection softening pressure relief measures. The authors processed and counted the mechanical parameters, as shown in Table 2.

3.2. Stress-Strain Curves of Coal Samples with Different Water Injection Softening States. To grasp the difference between different water injection softening pressure relief measures, this paper takes the following steps. Firstly, the stress-strain curves of typical bearing coal samples under natural conditions are analyzed (Figure 1). Secondly, based on the actual engineering background, the stress-strain curves of typical bearing coal samples before and after the implementation of different water injection softening and pressure relief measures are compared and analyzed.

3.2.1. Typical Natural State. The stress-strain curves of uniaxial compression tests of coal samples under the same state have good self-similarity. The loading process of coal samples analyzed in this paper experienced five stages: initial compaction stage, elastic deformation stage, plastic deformation stage, yield failure stage, and late failure stage.

Table 1: The sample number and state.

Sample state	Sample name	Sample number	Average moisture content
Dry state	Coal samples	$C_{0\text{-}1,2,3}$	0.00%
Natural state	Coal samples	$C_{1\text{-}1,2,3}$	2.64%
Saturated state	Coal samples	$C_{2\text{-}1,2,3}$	5.14%

3.2.2. Water Injection Softening Pressure Relief. Figure 1 is the stress-strain curve of coal samples under different water injection softening and pressure relief (changing water content). The test results show that the prepeak stress-strain curves of coal samples under different water injection softening control conditions have good similarity, while the characteristic parameters change. Specifically, the slope of the linear section before the peak is reduced, and the stress-strain curve after the peak is also different. The range of postpeak strain interval was positively correlated with water content. Figure 1 is reproduced from Zhang [26].

When the average moisture content of the coal sample is 0, 2.64%, and 5.14%, respectively, the average peak strength is 34.72 MPa, 21.33 MPa, and 19.16 MPa, respectively. The average peak strain is 0.03618, 0.02531, and 0.02791, respectively. The average elastic modulus is 4.25 GPa, 1.81 GPa, and 1.09 GPa, respectively. Compared with completely dry rock samples, the average peak strength decreased by 28.7% and 34.4%, respectively. The average peak strain decreased by 21.5% and 19.0%, respectively; the average elastic modulus decreased by 53.7% and 67.9%, respectively.

Comparing the test results, it can be seen that with the increase of water content, the peak strength of coal samples decreases, the peak strain decreases, and the elastic modulus decreases. However, the decreased amplitude decreased significantly with the increase in water content.

4. The Inversion of the Failure Process of Coal Sample Bearing Pressure Relief Measures Based on Energy Index

Based on the wide consensus of rockburst induced by energy release, the energy principle is generally used to analyze the energy evolution law of bearing rock. Simply through the calculation of energy theory, there is certain unity [24]. In this paper, the failure process of the bearing coal sample is inversed by the "true energy" index of the whole process of acoustic emission failure. The final mutual verification can illustrate the feasibility of the inversion of the failure process of the coal sample loaded by the pressure relief measures based on the energy index.

4.1. Energy Theorem. Take the uniaxial compression test of standard rock samples as an example. It is assumed that there is no heat exchange in the whole process; that is, the work done by the compression load on the rock sample is absorbed by the rock sample itself, and the total absorbed strain is denoted as U. In addition, the energy storage properties of rock samples have also been experimentally verified by many scholars. Therefore, most of the energy is stored in a releasable elastic strain energy U. The small part of residual energy is dissipated in the form of dissipated strain energy U^{d}, and the damage deformation is generated by bearing rock samples at the macrolevel. Its expression is

$$U = U^{\mathrm{e}} + U^{\mathrm{d}}. \tag{1}$$

The total strain energy absorbed by the bearing rock sample can be expressed as

$$U = \int \sigma_1 \mathrm{d}\varepsilon_1 = \sum_{i=0}^{n} \frac{1}{2}\left(\varepsilon_{1i+1} - \varepsilon_{1i}\right)\left(\sigma_{1i} + \sigma_{1i+1}\right), \tag{2}$$

$$U^{\mathrm{e}} = \frac{1}{2}\sigma_1 \varepsilon_1^{\mathrm{e}}. \tag{3}$$

According to Hooke's law,

$$U^{\mathrm{e}} = \frac{1}{2}\sigma_1 \varepsilon_1^{\mathrm{e}} \approx \frac{\sigma_1^2}{2E_0}. \tag{4}$$

In the formula, σ_1 and ε_1 are principal stress and strain values; σ_{1i} and ε_{1i} are the principal stress and strain corresponding to the i state curve; i is the data points; n is the total number of data points; $\varepsilon_1^{\mathrm{e}}$ is the elastic strain value; and E_0 is the initial elastic modulus.

4.2. Energy Distribution Characteristics of Coal Samples under Different Water Injection Softening Pressure Relief Measures. In this experiment, uniaxial compression tests were conducted on coal samples under different water injection softening and pressure relief conditions, and the energy evolution law was analyzed. Firstly, the energy distribution characteristics of coal samples in a natural intact state are drawn. In addition, to compare the differences between different water injection softening mechanisms, this paper analyzes the pressure relief measures of different water injection softening.

4.2.1. Typical Natural Integrity State. Figure 2 shows the relationship between stress, energy, and strain of natural coal samples under uniaxial conditions. The loading process of bearing coal sample experienced five stages: initial compaction stage (OA), elastic deformation stage (AB), plastic deformation stage (BC), yield failure stage (CD), and late failure stage (DE).

4.2.2. Water Injection Softening Pressure Relief. Figure 3 shows the relationship between stress, energy, and strain of coal samples under uniaxial drying and saturated conditions and summarizes the energy evolution curves under different conditions.

Compared with the typical natural state curve, the energy components of rock samples with different moisture contents also show corresponding changes in different stages of the stress-strain curve (initial compaction stage (OA), elastic deformation stage (AB), plastic deformation stage (BC), yield failure stage (CD), and late failure stage (DE)). The composition of the energy dissipation curve of rock

Table 2: Average mechanical parameters of coal samples under different water injection softening measures.

The corresponding working conditions	Sample state	Processing state	Sample number	Average peak strength (MPa)	Average peak strain	Average elastic modulus (GPa)
Blank experiment	Natural state	Blank untreated	$C_{0\text{-}1,2,3}$	21.33	0.02531	1.81
Water injection softening	Dry state	Complete drying	$C_{1\text{-}1,2,3}$	34.72	0.03618	4.25
	Saturated state	Fully saturated	$C_{2\text{-}1,2,3}$	19.16	0.02791	1.09

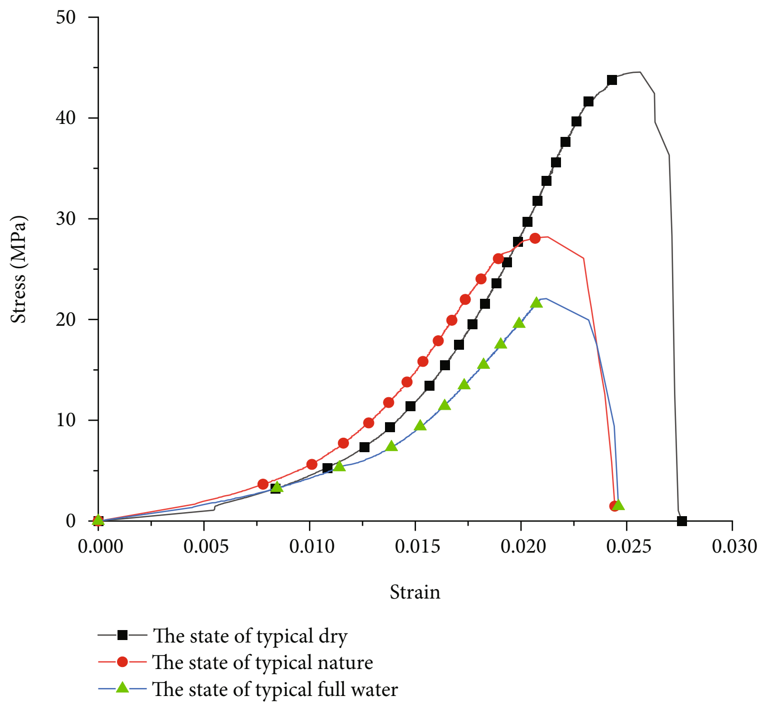

Figure 1: Stress-strain curves of rock samples in different water-bearing states.

samples in the dry state is essentially different from that in the natural and saturated state: the energy dissipation density curve rises throughout the drying state. Under natural and saturated conditions, the dissipation energy density curve showed an obvious or nonobvious downward trend and then increased.

4.3. Inversion of True Energy Acoustic Emission Parameters of Coal Samples under Different Water Injection Softening Measures. Due to the limited space, this paper only analyzes the failure process of "true energy" acoustic emission parameter inversion of coal sample underwater injection pressure relief. Figure 4 is the "true energy" acoustic emission evolution diagram of coal samples under dry state, natural state, and saturated state.

From the above images, it can be seen that the existence of water causes the "true energy" parameter to lag obviously. Due to the special structure of the coal sample, the influence of water on the coal sample affected the initial, middle, and late stages of loading and ran through the whole process.

4.4. Difference Analysis of Energy Evolution of Coal Samples under Different Water Injection Softening Measures. In this section, based on the energy distribution characteristics of coal samples under different water injection softening and pressure relief measures and the inversion of "true energy" acoustic emission parameters of coal samples under the same state, the energy evolution difference of coal samples under different water injection softening and pressure relief measures is comprehensively analyzed.

In the dry state, due to the natural pore-fracture dual-development structure of coal samples, the whole uniaxial loading process occurs at different scales (large, medium, and small) of pore-fracture closure, initiation, and expansion, accompanied by the disintegration and ejection of small blocks of coal samples. When it is in the low loading stress level stage, the pore-fracture closure occurs mainly (corresponding to the initial compaction stage). With the continuous increase of loading stress, the initiation and expansion of medium pores-cracks are dominant (corresponding to the elastic deformation stage and plastic deformation stage). There are occasional small pores and cracks closed during the plastic deformation stage, corresponding to the stress curve microadjustment time. After reaching the yield point, due to the extremely high loading stress, the pores and fractures at different scales in the previous

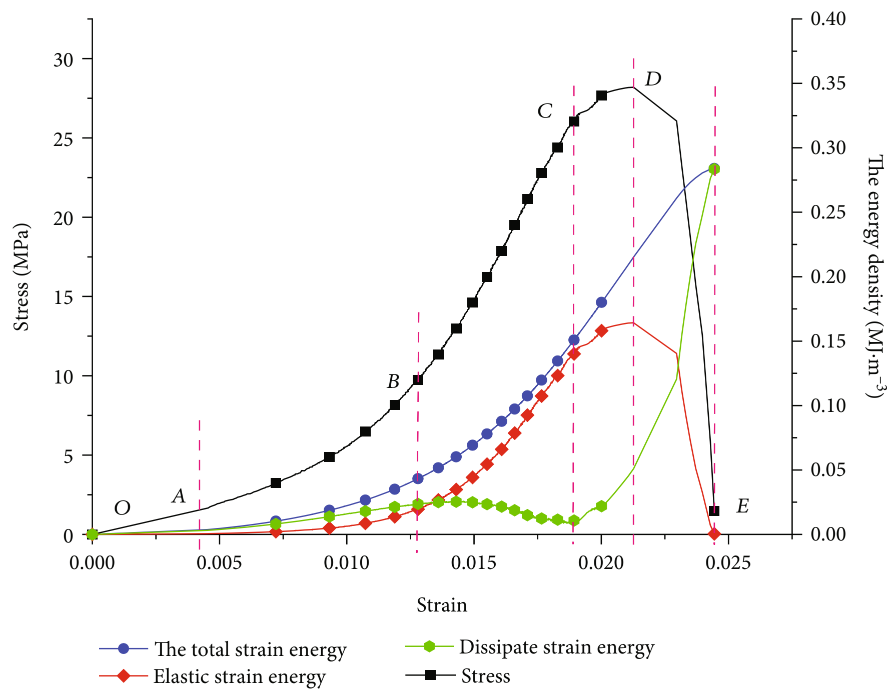

Figure 2: Natural state coal sample energy density curve.

sequence expand rapidly, the complete coal matrix is rapidly loaded and destroyed, and the dissipation energy increases rapidly in a short time (corresponding to the yield failure stage). After reaching the peak strength point, large-scale cracks penetrate directly, and the loading stress drops rapidly, forming a tensile-shear mixed failure mode, and the test ends (corresponding to the later stage of failure).

In the saturated state, water easily enters the natural initial internal structure of coal samples, forming a water-pore-fracture coupling medium. Water is filled in many large and medium pores-fractures and further coupled into a specific structure, which occupies a dominant position. There are still some pores-fractures at different scales alone. In this state, the closure, initiation, and expansion of pores and cracks at different scales still occur in the whole process of uniaxial loading. However, due to the participation of water, it shows special properties and occasionally the collapse and ejection of small blocks of coal samples. When it is in the stage of low loading stress level, due to the water-pore-fracture coupling medium and, at the same time, due to the incompressible water, only part of the macropore-fracture closure occurs mainly (corresponding to the initial compaction stage); with the continuous increase of loading stress, the water-pore-fracture coupling medium and the intact coal matrix form a relatively stable elastic body, which is characterized by the slow increase of stable storage elastic strain energy and dissipation strain energy (corresponding to the elastic deformation stage). When the loading stress reaches a higher stress level, the water in the pore-fracture shows a certain stiffness and can store more elastic strain energy. On the other hand, by increasing the pore water pressure and transferring the high stress to the complete coal matrix, the dissipation strain energy continues to decrease (corresponding to the plastic deformation stage). After reaching the yield point, the existence of high loading stress and high pore water pressure and the lubrication of water on the coal matrix greatly promote the rapid expansion of pores and fractures. The phenomenon of rapid rebound and rise of dissipative strain energy in a short time (corresponding to the yield failure stage) occurs. After reaching the peak strength point, larger cracks run through directly. At this time, the loading stress drops rapidly, forming a tensile-shear mixed failure mode, and the test ends (corresponding to the later stage of failure).

5. Analysis of the Shock Tendency Difference of Coal Samples under Different Water Injection Softening Measures and the Failure Reason of Failure Precursor Identification

5.1. Difference Analysis of Energy Evolution of Coal Samples under Different Water Injection Softening Measures. Based on the existing shock tendency criterion of coal samples, the shock difference of coal samples under different water injection softening measures was analyzed. The criterion requires the standard shape. In this paper, the square sample is used, which cannot be analyzed according to the correlation index. However, according to the increase or decrease trend of the four indicators, the results of shock tendency are comprehensively evaluated. Table 3 lists the shock indicators of coal samples under different conditions.

From the final impact results (Table 3), the water injection pressure relief state can well meet the conditions and reduce the impact tendency of the overall coal sample. This meets the concept of rockburst prevention.

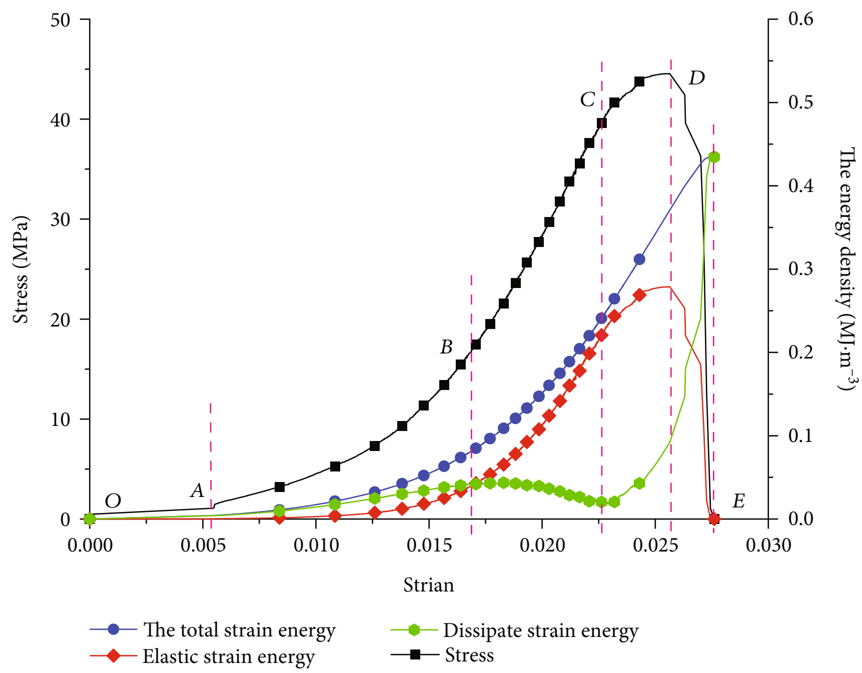

(a) Dry state coal sample energy density curve

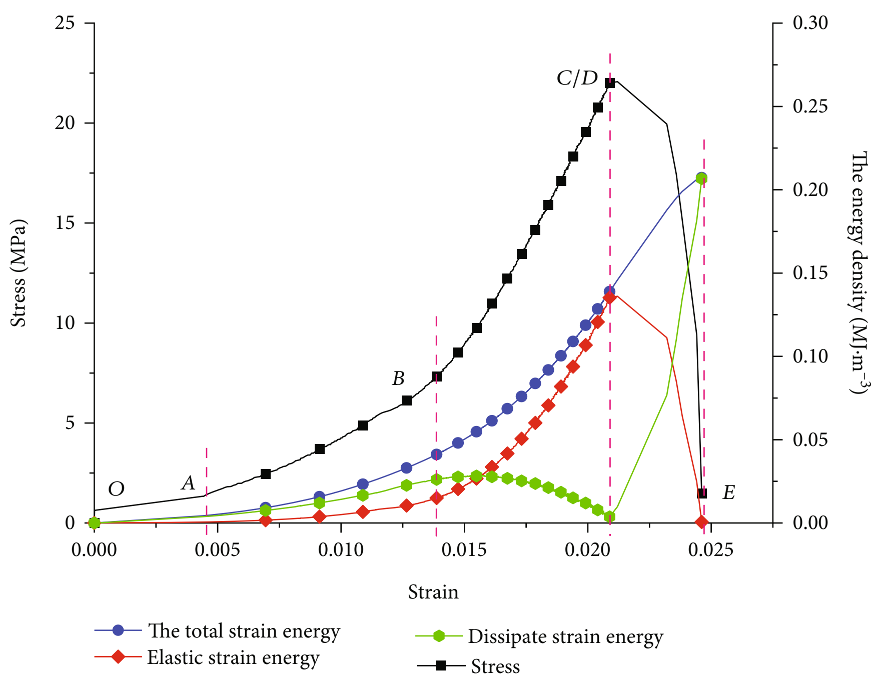

(b) Saturated state coal sample energy density curve

FIGURE 3: Relationship between stress, energy, and strain of rock samples under uniaxial conditions of different water-bearing states.

5.2. Credibility Analysis of Failure Precursor Discrimination. The overall water injection pressure relief conforms to the concept of rockburst prevention, which can effectively weaken the impact tendency of coal samples. However, impact tendency is only an indicator of rockburst, and other influencing factors are also very important. Therefore, we need to accurately identify the characteristic parameters in the process of pregnant disaster signals from the perspective of prediction.

It can be seen from the variation trend of the stress-strain whole process that the refined calculation of the yield failure stage is a necessary condition for accurately predicting the failure of bearing coal samples at the laboratory scale. Other domestic scholars have studied the curves of the whole process of energy evolution of a large number of rocks and obtained more consistent discriminant conditions. Dissipative strain energy is in a stable fluctuation or rapid decline range, which

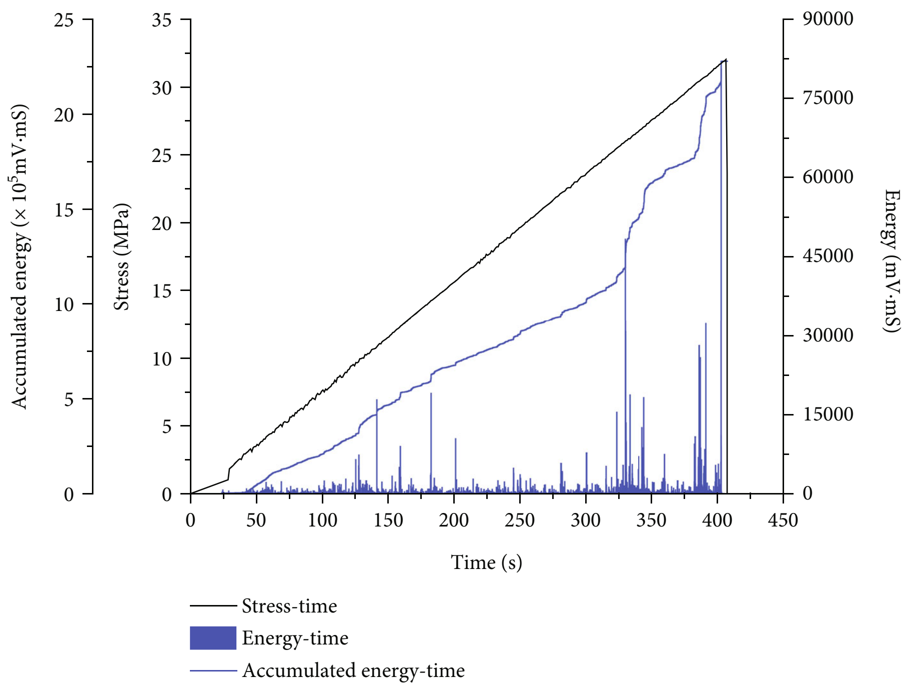

(a) Whole evolution of "true energy" acoustic emission of coal samples under dry state

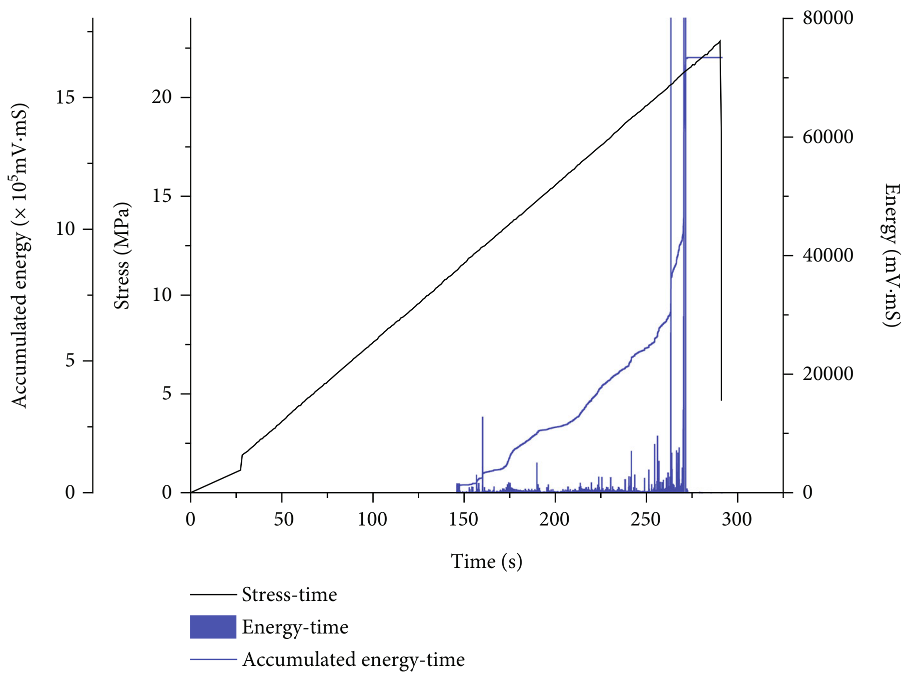

(b) Whole evolution of "true energy" acoustic emission of coal samples under natural state

Figure 4: Continued.

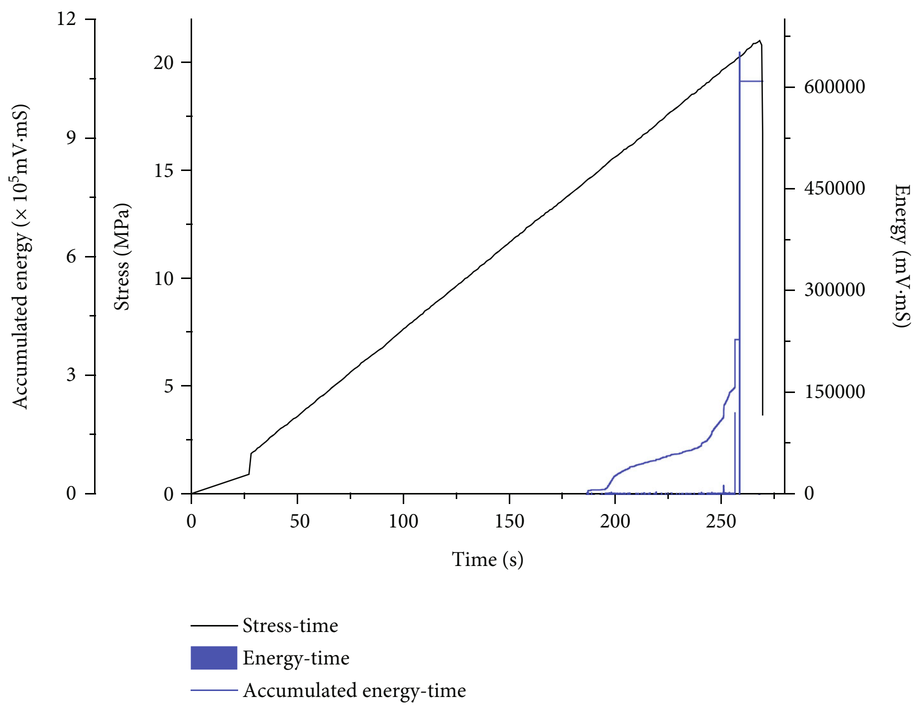

(c) Whole evolution of "true energy" acoustic emission of coal samples under saturated state

Figure 4: The whole evolution of "true energy" acoustic emission of coal samples under different conditions.

Table 3: Comparison of shock tendency index criterion of coal samples under different water injection conditions.

Sample state	Dynamic failure time	Shock energy index	Elastic energy index	Uniaxial compressive strength	Results of the comprehensive evaluation
Dry state	926	28.440	1.048	32.040	High
Natural state	818	2.830	1.580	22.848	Mid
Saturated state	1440	2.008	6.135	21.016	Low

means that the rock enters the yield failure stage. Accurate early warning of the yield stage can be attempted by identifying other sensitive parameter signals in this region.

Coal has a special structure. We found that both natural coal samples and saturated coal sample underwater injection pressure relief met the prediction conditions. The dry coal sample does not meet the prediction conditions; that is, it is unable to accurately pick up the precursor signal of pregnancy, so it is unable to accurately predict the coal sample damage. The natural coal samples on a laboratory scale are in the state of adsorption in the air after sampling. Due to the influence of self-weight or mining disturbance, the coal pore-fracture near the deep working face tends to have low water content, so it is difficult to predict and prevent, which has a great influence on the reasonable control of water injection pressure relief parameters.

6. Conclusions

In this paper, the difference in the energy evolution process of bearing coal samples under different water injection softening and pressure relief conditions is revealed through uniaxial compression experiments. In addition, it is attempted to analyze the reasons why it is difficult to accurately predict the occurrence of rockburst in coal roadways with research methods. This provides a theoretical basis for the subsequent scientific and reasonable pressure relief measures and parameters and ultimately achieves the purpose of preventing rock bursts. The main conclusions are as follows:

(1) Water injection softening can significantly affect the mechanical parameters of coal samples. Compared with fully dry coal samples, when the average moisture content of coal samples was 0, 2.64%, and 5.14%, the average peak strength decreased by 28.7% and 34.4%, respectively. The average peak strain decreased by 21.5% and 19.0%, respectively. The average elastic modulus decreased by 53.7% and 67.9%, respectively

(2) The whole process stress-strain curves of coal samples under different water injection softening measures also experienced the initial compaction stage, elastic deformation stage, plastic deformation stage, yield failure stage, and late failure stage. In this paper,

the failure process of the bearing coal sample is inversed by the "true energy" index of the whole process of acoustic emission failure, forming a theoretical basis for mutual support. This shows the feasibility of the failure process inversion of different bearing coal samples based on the "true energy" index

(3) Coal has a special structure. We found that both natural and saturated water injection softening unloading coal samples can meet the failure prediction conditions. The water injection pressure relief coal sample under dry conditions is not satisfactory; that is, it is unable to accurately pick up the precursor signal of pregnancy disaster and accurately predict the failure of coal samples. The natural state of coal samples at the laboratory scale is in the state after sampling and adsorption in the air, while the coal near the deep working face of the mine is often in the state of low water content due to the development of pores and fissures and affected by gravity or mining disturbance. Therefore, the prediction and prevention of rockburst are difficult, which has a great influence on the reasonable control of water injection pressure relief parameters

Data Availability

The data used to support the findings of this study are available from the corresponding author upon request.

Conflicts of Interest

No conflict of interest exists in the submission of this manuscript.

Authors' Contributions

The manuscript is approved by all authors for publication.

Acknowledgments

The study has been supported by the basic research program of Natural Science Foundation of Shaanxi Province (No. S2019-JC-LH-QY-SM-0102), the National Natural Science Foundation of China (No. 51904227), and the Key Research and Development Program of Shaanxi Province (No. 2018ZDXM-SF-018). Support from these agencies is gratefully acknowledged.

References

[1] H. Xu, X. Lai, S. Zhang et al., "Multiscale intelligent inversion of water-conducting fractured zone in coal mine based on elastic modulus calibration rate response and its application-a case study of Ningdong mining area," *Lithosphere*, vol. 2021, article 7657143, 16 pages.

[2] L. Dong, Q. Hu, X. Tong, and Y. Liu, "Velocity-free MS/AE source location method for three-dimensional hole- containing structures," *Engineering*, vol. 6, no. 7, pp. 827–834, 2020.

[3] L. Dai, Y. Pan, Z. Li et al., "Quantitative mechanism of roadway rockbursts in deep extra-thick coal seams: theory and case histories," *Tunnelling and Underground Space Technology*, vol. 111, p. 103861, 2021.

[4] J. Xin, L. Liu, L. Xu, J. Wang, P. Yang, and H. Qu, "A preliminary study of aeolian sand-cement-modified gasification slag-paste backfill: fluidity, microstructure, and leaching risks," *Science of the Total Environment*, vol. 830, article 154766, 2022.

[5] L. M. Dou, Z. L. Mu, Z. L. Li, A. Y. Cao, and S. Y. Gong, "Research progress of monitoring, forecasting, and prevention of rockburst in underground coal mining in China," *International Journal of Coal Science & Technology*, vol. 1, no. 3, pp. 278–288, 2014.

[6] W. Cai, L. Dou, G. Si et al., "A new seismic-based strain energy methodology for coal burst forecasting in underground coal mines," *International Journal of Rock Mechanics and Mining Sciences*, vol. 123, article 104086, 2019.

[7] Q. Liu, J. Chai, S. Chen, D. Zhang, Q. Yuan, and S. Wang, "Monitoring and correction of the stress in an anchor bolt based on pulse pre- pumped brillouin optical time domain analysis," *Energy Science & Engineering*, vol. 8, no. 6, pp. 2011–2023, 2020.

[8] D. Bakun-Mazor, Y. H. Hatzor, and W. S. Dershowitz, "Modeling mechanical layering effects on stability of underground openings in jointed sedimentary rocks," *International Journal of Rock Mechanics and Mining Sciences*, vol. 46, no. 2, pp. 262–271, 2009.

[9] R. Xue, Z. Liang, N. Xu, and L. Dong, "Rockburst prediction and stability analysis of the access tunnel in the main powerhouse of a hydropower station based on microseismic monitoring," *International Journal of Rock Mechanics and Mining Sciences*, vol. 126, article 104174, 2020.

[10] Y. Wang, C. A. Tang, L. Tang et al., "Microseismicity characteristics before and after a rockburst and mechanisms of intermittent rockbursts in a water diversion tunnel," *Rock Mechanics and Rock Engineering*, vol. 55, no. 1, pp. 341–361, 2022.

[11] G. Cheng, T. Ma, C. Tang, H. Liu, and S. Wang, "A zoning model for coal mining - induced strata movement based on microseismic monitoring," *International Journal of Mining Science and Technology*, vol. 94, pp. 123–138, 2017.

[12] X. Lai, Y. Yang, and L. Zhang, "Research on structural evolution and microseismic response characteristics of overlying strata during repeated mining of steeply inclined and extra thick coal seams," *Lithosphere*, vol. 2021, no. Special 4, article 8047321, 2021.

[13] X. Lai, H. Xu, J. Chen et al., "Research on energy dissimilation characteristics and control method of sandwiched rock pillar by steeply inclined mining," *Journal of Mining & Safety Engineering*, vol. 38, no. 3, pp. 429–438, 2021, (In Chinese).

[14] J. F. Pan, S. H. Liu, J. M. Gao, X. Sun, Y. Xia, and Q. Wang, "Prevention theory and technology of rock burst with distinguish dynamic and static load sources in deep mine roadway," *Journal of China Coal Society*, vol. 45, no. 5, pp. 1607–1613, 2020, (In Chinese).

[15] P. A. N. Junfeng, "Theory of rock burst start-up and its complete technology system," *Journal of China Coal Society*, vol. 44, no. 1, pp. 173–182, 2019, (In Chinese).

[16] Y. Zhao, C. L. Wang, L. Ning, H. F. Zhao, and J. Bi, "Pore and fracture development in coal under stress conditions based on nuclear magnetic resonance and fractal theory," *Fuel*, vol. 309, article 122112, 2022.

[17] Y. Zhao, C. L. Wang, and J. Bi, "Analysis of fractured rock permeability evolution under unloading conditions by the model of

elastoplastic contact between rough surfaces," *Rock Mechanics and Rock Engineering*, vol. 53, no. 12, pp. 5795–5808, 2020.

[18] L. Xing-ping, L. Xiao-dong, W. Yong-ping, Z. Yong, and L. Zhao-hai, "Experiment on dynamical damage of overburden-rock media at various scale mined-out area in excavation disturbed zone," *Journal of China Coal Society*, vol. 32, no. 9, pp. 902–904, 2007, (In Chinese).

[19] M. Cai, P. K. Kaiser, and C. D. Martin, "Quantification of rock mass damage in underground excavations from microseismic event monitoring," *International Journal of Rock Mechanics and Mining Sciences*, vol. 38, no. 8, pp. 1135–1145, 2001.

[20] Y. D. Jiang, Y. S. Pan, F. X. Jiang, L. M. Dou, and Y. Ju, "State of the art review on mechanism and prevention of coal bumps in China," *Journal of China Coal Society*, vol. 39, no. 2, pp. 205–213, 2014, (In Chinese).

[21] S. J. Gibowicz and A. Kijko, *An Introduction to Mining Seismology [M]*, Academic Press, New York, 1994.

[22] A. Wang, Y. Pan, and B. Zhao, "Coupling vibration characteristics of rock mass and energy-absorption bolt and its anti-impact mechanism," *Journal of China Coal Society*, vol. 41, no. 11, pp. 2734–2742, 2016, (In Chinese).

[23] J. Liu, X. Feng, Y. Li, S.-d. Xu, and Y. Sheng, "Studies on temporal and spatial variation of microseismic activities in a deep metal mine," *International Journal of Rock Mechanics and Mining Sciences*, vol. 60, pp. 171–179, 2013.

[24] W. Liang, Y. Zhao, and X. Suguo, "Study on the theory of in-situ solution mining," *Journal of Taiyuan University of Technology*, vol. 43, no. 3, pp. 382–387, 2012, (In Chinese).

[25] H. Xie, R. Peng, and J. Yang, "Energy dissipation of rock deformation and fracture," *Chinese Journal of Rock Mechanics and Engineering*, vol. 23, no. 21, pp. 3565–3570, 2004, (In Chinese).

[26] F. Zhang, "Analysis on the difference of energy evolution in the process of energy storage failure of strong coal rush rock samples under different adaptive modification regulation measures," *Shock and Vibration*, vol. 2022, Article ID 1471945, pp. 1–11, 2022.